Title

A heteromeric Texas coral snake toxin targets acid-sensing ion channels to produce pain

Journal

Nature, 479(7373)

ISSN

0028-0836

Authors

Bohlen, Christopher J

Chesler, Alexander T

Sharif-Naeini, Reza

et al.

Publication Date

2011-11-01

DOI

10.1038/nature10607

Peer reviewed

Published in final edited form as:

Nature. ; 479(7373): 410–414. doi:10.1038/nature10607.

A heteromeric Texas coral snake toxin targets acid-sensing ion channels to produce pain

Christopher J. Bohlen[1,*], **Alexander T. Chesler**[1,*], **Reza Sharif-Naeini**[2], **Katalin F. Medzihradszky**[3], **Sharleen Zhou**[4], **David King**[4], **Elda E. Sánchez**[5], **Alma L. Burlingame**[3], **Allan I. Basbaum**[2], and **David Julius**[1]

[1]Department of Physiology, University of California, San Francisco, CA 94158-2517, USA

[2]Department of Anatomy, University of California, San Francisco, CA 94158-2517, USA

[3]Department of Pharmaceutical Chemistry, University of California, San Francisco, CA 94158-2517, USA

[4]Howard Hughes Medical Institute Mass Spectrometry Laboratory, University of California, Berkeley, CA 94720-3202, USA

[5]National Natural Toxins Research Center and Department of Chemistry, Texas A&M University-Kingsville, Texas 78363, USA

Abstract

Natural products that elicit discomfort or pain represent invaluable tools for probing molecular mechanisms underlying pain sensation[1]. Plant-derived irritants have predominated in this regard, but animal venoms have also evolved to avert predators by targeting neurons and receptors whose activation produces noxious sensations[2-6]. As such, venoms provide a rich and varied source of small molecule and protein pharmacophores[7,8] that can be exploited to characterize and manipulate key components of the pain-signaling pathway. With this in mind, we carried out an unbiased *in vitro* screen to identify snake venoms capable of activating somatosensory neurons. Venom from the Texas coral snake (*Micrurus tener tener*), whose bite produces intense and unremitting pain[9], excited a large cohort of sensory neurons. The purified active species (MitTx) consists of a heteromeric complex between Kunitz- and phospholipase A2-like proteins that together function as a potent, persistent, and selective agonist for acid-sensing ion channels (ASICs), showing equal or greater efficacy when compared with acidic pH. MitTx is highly selective for the ASIC1 subtype at neutral pH; under more acidic conditions (pH < 6.5), MitTx

Correspondence and requests for materials should be addressed to D.J. (david.julius@ucsf.edu).

*denotes equal contribution

AUTHOR CONTRIBUTIONS: C.B. and A.C initiated the screen, performed experiments, and analyzed data. R.S-N. and A.I.B. performed and analyzed behavioral experiments and spinal cord histology. K.F.M., A.L.B, S.Z., and D.K. determined partial protein sequences and performed mass spectrometry measurements. E.S. provided snake venom and tissue. C.B., A.C, and D.J. wrote the manuscript with discussion and contribution from all authors. D.J. supervised the project and provided guidance throughout.

GenBank accession numbers for MitTxα, MitTxβ, and MttPLA2 cDNA sequences are JN613325, JN613326, and JN613327 respectively.

The authors declare no competing financial interests.

massively potentiates (>100-fold) proton-evoked activation of ASIC2a channels. These observations raise the possibility that ASIC channels function as coincidence detectors for extracellular protons and other, as yet unidentified, endogenous factors. Purified MitTx elicits robust pain-related behavior in mice via activation of ASIC1 channels on capsaicin-sensitive nerve fibers. These findings reveal a mechanism whereby snake venoms produce pain, and highlight an unexpected contribution of ASIC1 channels to nociception.

To identify novel toxins that activate nociceptors, we screened venoms from a variety of snake species for their ability to depolarize specific subpopulations of somatosensory neurons using calcium imaging as a functional readout. Among these, venom from the Texas coral snake, which elicits intense acute pain associated with local edema and inflammation[9], produced clear and robust activation of most, but not all, neurons cultured from trigeminal ganglia (TG) of newborn (P0-P2) rats (Fig 1a, b). In contrast, coral snake venom had no effect on sympathetic neurons cultured from superior cervical ganglia (not shown).

We next fractionated the crude venom using reversed-phase chromatography (Supplementary Fig. 1) to identify the active component(s). No single fraction excited sensory neurons, but when re-pooled the individual fractions fully reconstituted activity observed with the crude venom, suggesting a requirement for multiple components. Pair-wise analysis of these fractions identified two components (MitTxα and MitTxβ), which could be purified to near-homogeneity with subsequent chromatographic steps, as assessed by gel filtration chromatography, SDS-PAGE, and mass spectrometry (not shown). These two toxins together proved necessary and sufficient to recapitulate activity of the crude venom. Mass spectrometry and N-terminal Edman sequencing showed that both MitTxα and MitTxβ are proteinaceous in nature, and partial amino acid sequences derived from these analyses were used to clone full-length cDNAs from the coral snake venom gland. The deduced amino acid sequences revealed patterns of cysteine residues that classify MitTxα and MitTxβ as Kunitz type and phospholipase A2 (PLA2)-like proteins, respectively (Fig. 1c and Supplementary Fig. 1). Indeed, these families of cysteine-rich disulfide bonded proteins are prevalent components of various snake venoms[8], and in some cases have been shown to form biochemical complexes[10].

To determine whether MitTxα and MitTxβ form a heteromeric complex, we used isothermal titration calorimetry to detect any such molecular interaction. We observed a substantial exothermic reaction ($\Delta H = -18.9 \pm 1.3$ kcal mol^{-1}) upon mixing, resulting from a high affinity binding event ($K_d = 12.2 \pm 3.1$ nM) with 1:1 stoichiometry ($n = 1.02 \pm 0.05$) (Fig. 1d). These biochemical results are consistent with our physiological analysis showing that neither MitTxα nor MitTxβ activated sensory neurons alone, whereas a robust and immediate rise in intracellular calcium was produced when both components were added simultaneously or sequentially (in either order) (Fig. 1e). Moreover, even a brief washout period between sequential applications prevented activation (Fig. 1f), suggesting that only the MitTx α/β complex forms a persistent and productive interaction with its physiological target.

Having defined the molecular nature of the toxin components, we next sought to elucidate its mechanism of action on sensory neurons. As the MitTxβ component lacks critical

catalytic residues normally found in the active site of related PLA2 enzymes[11] phospholipase activity seemed unlikely to contribute to neuronal excitation. In fact, we failed to detect PLA2 activity associated with any component, together or alone (Supplementary Fig. 1), suggesting that the toxin is not producing neuronal depolarization simply by degrading the plasma membrane (consistent with the observed action on a subset of somatosensory neurons). It is possible that this toxin maintains some lipid-binding character from its PLA2 lineage, which could aid the toxin in effecting neuronal depolarization.

To gain clues as to the cellular mechanism of toxin action, we performed a detailed biophysical analysis of toxin-evoked responses. Whole cell patch clamp recordings showed that purified MitTx α/β complex (hereafter referred to as MitTx) produced robust currents in a subset of trigeminal neurons. These currents were characterized by a linear current-voltage relationship and high permeability to Na^+ versus Cs^+ ions (P_{Na^+}:P_{Cs^+} = 10.1 ± 1.0, Fig. 2a). In searching for potential molecular targets expressed by sensory neurons, we next investigated members of the ASIC family, which exhibit properties consistent with these parameters[12-14]. We expressed various ASIC subtypes in *Xenopus* oocytes and measured toxin-evoked electrophysiological responses. Figure 2 shows that application of MitTx produced large and sustained membrane currents in oocytes expressing the ASIC1b subtype (Fig. 2b, c). Consistent with our results using cultured neurons, neither MitTxα nor MitTxβ was active on its own, but robust responses were evoked when both components were applied to oocytes, whether pre-mixed or mixed *in situ*. Furthermore, the ENaC/ASIC blocker, amiloride, abolished these responses. When applied at maximal concentration, MitTx elicited responses exceeding those produced by saturating doses of extracellular protons. Whereas protons elicit very transient responses, those evoked by toxin were dramatically prolonged, reflecting both lack of desensitization and slow reversibility after washout (Fig 2c).

Among ASIC subtypes, the most robust toxin-evoked responses were observed with ASIC1a or 1b based on potency (EC_{50} = 9.4 ± 1.3 and 23 ± 3.6 nM, respectively), efficacy (relative to protons), and persistence of action (Fig. 2d and Supplementary Fig. 2). MitTx must interact with an extracellular region of the channel since responses were observed in the outside-out (but not inside-out) configuration when toxin was applied to patches excised from ASIC1a-expressing CHO cells (not shown). Moreover, at least for ASIC1a, toxin potency (9 nM) is likely limited by the affinity of α/β complex formation (12 nM, Fig. 1d) and not by the toxin-channel interaction itself.

The ASIC3 subtype was also MitTx sensitive, but required ∼100-fold higher toxin concentration to achieve half-maximal activation (EC_{50} = 830 ± 250 nM). This lower potency was accompanied by relatively slow activation and fast washout kinetics compared to those observed with ASIC1a or 1b (Supplementary Fig. 2). By comparison, ASIC2a showed very weak activation by toxin, never achieving more than 10% efficacy compared to proton-evoked responses (Fig. 2d, e). Despite this anemic response, the toxin produced a remarkable potentiation of acid-evoked currents, greatly enhancing both potency and efficacy of protons (Fig. 2e, f). Indeed, as the extracellular pH drops below neutrality, the toxin itself becomes an excellent ASIC2a agonist, essentially enhancing the potency of

protons by three orders of magnitude. Two remaining ASIC family members, 2b and 4, do not produce proton-activated channels on their own, and we did not observe MitTx-evoked responses in oocytes expressing these subtypes. As a further testament to toxin specificity, MitTx produced neither activation nor persistent inhibition when applied to a diverse range of cloned ion channels, including voltage-gated, ENaC, TRP, P2X, or 5-HT_3 channels (Supplementary Fig. 3). Additionally, MitTx activated the same percentage of trigeminal neurons cultured from wild type or TRPV1/TRPM8/TRPA1 triple knockout mice (Supplementary Fig. 4).

Micrurus tener tener is not the only coral snake species to express ASIC-activating toxins; venom from the Brazilian coral snake (*Micrurus frontalis*) activated a similar cohort of cultured rat trigeminal sensory neurons, or oocytes expressing cloned ASIC1a channels (Supplementary Fig. 5). Interestingly, ASIC1a is also targeted by a peptide toxin from tarantula (PcTx1), but in this case, the toxin serves as a functional antagonist of proton-evoked responses by locking the channel in a desensitized state[15,16]. ASIC1a channels blocked by PcTx1 could not be activated by MitTx, and MitTx-activated channels could not be blocked by PcTx1 (Fig. 2g, h), suggesting physical or functional occlusion of toxin action.

We next used patch clamp recording methods to determine whether MitTx-evoked neuronal responses exhibit properties consistent with an ASIC-mediated mechanism. Sensory neurons show both transient and sustained proton-evoked responses, with the former being mediated primarily by ASIC channels and the latter by capsaicin-sensitive TRPV1 channels[17,18]. We found that all MitTx-sensitive neurons exhibited transient responses to extracellular protons (pH 4), toxin responses were blocked by amiloride and eliminated in Na^+-free perfusate, and the relative magnitude of toxin-to-proton evoked responses resembled those observed in transfected mammalian (CHO) cells expressing the cloned rat ASIC1a or 1b channels (Fig. 3a, b). Further evidence that ASIC1 is the predominant target of MitTx came from analysis of electrophysiological responses in TG neurons from newborn ASIC1- or ASIC3-deficient mice[19,20]. The percentage of toxin-sensitive cells from $ASIC1^{-/-}$ mice was greatly diminished compared to wild type or $ASIC3^{-/-}$ animals (Fig. 3c, d). Using calcium imaging to sample a larger population of neurons, we found that responses to moderate toxin concentrations (20 nM) were completely absent in TG cultures from $ASIC1^{-/-}$ mice, but unperturbed in those from $ASIC3^{-/-}$ animals (Fig. 3e-g). Only at substantially higher toxin concentrations (600 nM; exceeding the EC_{50} for ASIC1 by ≥ 30-fold) did we record a relatively small subset of toxin-sensitive neurons in $ASIC1^{-/-}$ cultures. These residual toxin responses were eliminated when depolarization-evoked calcium influx was suppressed in Na^+-free perfusate (Supplementary Fig. 6), consistent with Ca^{2+}-impermeant ASIC2 and/or 3 subtypes accounting for the activity. Indeed, $ASIC3^{-/-}$ cultures showed a small, but significant diminution in the percentage of neurons responding to 600 nM MitTx (Fig. 3g).

The role of ASIC channels in pain has focused primarily on ASIC3 given its somatosensory neuron-specific pattern of expression[13]. MitTx provides a novel tool with which to determine whether ASIC1 and ASIC1-expressing neurons also contribute to nociception. Injection of MitTx into the hind paw of wild type mice produced robust nocifensive (pain-related) behavior scored as a characteristic licking response (Fig. 4a). In the same animals,

we observed abundant Fos protein expression in superficial laminae of the ipsilateral dorsal spinal cord, demonstrating engagement of nociceptive pathways (Fig. 4b). These responses were diminished in ASIC1-deficient mice, but persisted in ASIC3$^{-/-}$ animals, demonstrating a predominant contribution of ASIC1 channels to toxin-evoked nocifensive behavior.

Are these responses mediated through a well-characterized population of nociceptors? To address this question, we first examined MitTx-sensitive neurons for expression of relevant molecular markers of subpopulations of nociceptors. One third of toxin-sensitive neurons expressed TRPV1, whereas a much smaller group (11%) were labeled by isolectin B4, which in mice marks a population of TRPV1-negative, non-peptidergic C-fibers. The majority (53%) of toxin-sensitive neurons immunostained for the NF200 neurofilament, placing them among the subpopulation of medium-to-large diameter neurons with myelinated axons (Fig. 4c). As many large diameter sensory neurons respond to innocuous mechanical stimulation, these histological results suggest that functional ASIC1 channels are expressed by both nociceptive and non-nociceptive somatosensory neurons. Next, we asked whether MitTx elicits nocifensive responses in mice in which the central terminals of TRPV1-expressing nociceptors have been selectively ablated through spinal (intrathecal) injection of capsaicin[21]. Indeed, these animals showed a complete loss of toxin-evoked behavior and Fos immunoreactivity in the spinal cord (Fig. 4d), demonstrating that the painful effects of MitTx are mediated entirely by a relatively small cohort (less than a third) of ASIC1-expressing nerve fibers.

Bites and stings from venomous creatures produce pain to ward off predators[2-4], and thus it stands to reason that some toxins have evolved to target efficiently elements of the pain pathway. In fact, bites from some coral snake species are well known to elicit excruciating pain requiring hospitalization and administration of opiate analgesics[9,22]. Our results show that MitTx has evolved from Kunitz type and PLA2-like protein scaffolds to evoke intense and persistent pain by producing robust and long-lasting activation of ASIC1 channels on the nociceptive terminals of mammalian, avian, or serpentine predators. Just as capsaicin and some spider toxins highlight the importance of TRPV1 in pain sensation, so MitTx implicates ASIC1 channels in this protective sensory modality, further illustrating the power of natural products in identifying key components and therapeutic targets of nociceptive signaling pathways.

In light of its selective expression within somatosensory ganglia and a well-documented contribution to ischemic pain, studies of ASIC channels in nociception have focused primarily on the ASIC3 subtype[13,23-26]. The extremely persistent (non-desensitizing) and selective nature of MitTx action has enabled us to functionally isolate ASIC1 channels and reveal their contribution to pain sensation through the activation of TRPV1-expressing neurons. This nociceptor population has been suggested to constitute a ‘labeled line’ required for acute detection of noxious heat, as well as tissue injury-evoked pain hypersensitivity[1,21]. Activation of ASIC1 on these nerve fibers may contribute to the non-TRPV1 component of proton-mediated sensitization associated with tissue acidosis and inflammatory pain. ASIC1 is also expressed by non-nociceptive somatosensory neurons, as well as other neural and non-neural tissues[14,20,24,27]. Thus, MitTx represents a novel class of pharmacological probes with which to elucidate the contributions of ASIC channels to a

variety of physiological processes. Finally, it is intriguing that MitTx can potentiate proton efficacy at some ASIC subtypes (most notably ASIC2a) by two or three orders of magnitude. That is to say, MitTx reveals the fact that protons only activate ASIC2a channels to <10% of maximal open probability, suggesting that protons do not exploit the full potential of ASIC2a as a ligand-gated channel. Although small FMRF-amide-like peptides have been shown to potentiate proton-gated currents through ASIC1 and ASIC3 (primarily by slowing desensitization)[25,28], the profound enhancing effects mediated by MitTx hint at the existence of other, more potent physiological modulators for this class of excitatory channels.

Methods Summary

MitTxα and MitTxβ were purified from crude *Micrurus tener tener* venom (National Natural Toxin Research Center, Texas A&M University-Kingsville, Texas, USA) using multiple reversed-phase HPLC steps and purity assessed by mass spectrometry and gel filtration chromatography. Partial toxin sequences were determined by Edman degradation and/or *de novo* MS/MS sequencing analysis and used to design degenerate primers for cloning full-length MitTxα and MitTxβ cDNAs from *M. t. tener* venom gland library. PcTx1 was purified from *Psalmopoeus cambridgei* venom (SpiderPharm Inc.) and *Micrurus frontalis* venom was purchased from Sigma. ASICs were cloned from rat trigeminal ganglion or brain cDNA libraries (except mouse ASIC2b, which was provided by Michael Welsh, University of Iowa, IA). For ITC experiments, MitTxβ (3 to 10 μM) was titrated into MitTxα (0.3 to 1 μM) at 15 °C. Molecular biology, neuronal dissociation, cell culture, calcium imaging, and electrophysiological experiments were conducted essentially as described[6]. P_{Na^+} / P_{Cs^+} was determined by substituting observed reversal potential into the Goldman-Hodgkin-Katz voltage equation. Animal experiments were approved by the UCSF Institutional Animal Care and Use Committee and conducted in accordance with the National Institutes of Health (NIH) Guide for the Care and Use of Laboratory Animals and the recommendations of the International Association for the Study of Pain as described[5,21]. Both behavioral and histological experiments were conducted and scored with the experimenter blind to genotype.

Methods

Toxin Purification

Crude *Micrurus tener tener* venom, pooled from multiple specimens, was provided by the National Natural Toxins Research Center, Texas A&M University-Kingsville, Texas, USA. Lyophilized venom was dissolved in water to 100 mg ml^{-1}, diluted 30-fold into 20% acetonitrile containing 0.1% trifluoroacetic acid (TFA), filtered through 0.1 μm centrifugal filter unit (Millipore) and fractionated by reversed-phase HPLC. Up to 20 mg venom was loaded onto a semi-preparative C18 column (Vydac model 218TP510), and eluted with a 20 min linear gradient (18-36% acetonitrile; 3 ml min^{-1}). Fractions containing predominantly MitTxα were diluted two-fold with 0.1% TFA, injected onto an analytical PLRP-S column (Varian PL1512-5501), and separated with an 8 minute linear gradient (27-34% acetonitrile; 0.8 ml min^{-1}); MitTxα containing fractions were again diluted, injected onto an analytical C18 column (Vydac 218TP54), and separated with a 20 minute linear gradient (18-36%

acetonitrile; 0.8 ml min^{-1}). MitTxβ fractions from the semi-preparative run were diluted, applied to an analytical C18 column (Vydac 218TP54), and separated with a 7 minute linear gradient (30-36% acetonitrile; 0.8 ml min^{-1}). All HPLC buffers contained 0.1% TFA, and all purifications were performed at room temperature (RT). Purified fractions were lyophilized then dissolved in water, aliquoted, and stored at -80 °C. Protein concentration was determined using calculated extinction coefficient at 280 nm (http://us.expasy.org/tools/protparam.html).

PcTx1 was purified from *Psalmopoeus cambridgei* venom (SpiderPharm Inc.) using two sequential HPLC steps consisting of 114 minute linear gradient (0-54% acetonitrile on a semi-preparative C18 column) followed by the same gradient on an analytical C18 column (as above). *Micrurus frontalis* venom was purchased from Sigma.

Sequence Determination

Toxin masses were determined using a Bruker Apex III ESI-Q-FTICR mass spectrometer, and the N-terminal sequencing was performed on an Applied Biosystems 492 Procise Sequencer previously described[6]. Edman degradation yielding partial sequence (NLNQFRLMIKCTNDRV…) for MitTxβ, but not MitTxα due to modified (pyroglutamic acid) N-terminus. Partial MitTxα sequence was determined *de novo* by MS/MS sequencing analysis. After reduction under acidic conditions (0.1% formic acid, 5mM TCEP for 24 hrs at 37 °C) MitTxα was subjected to CID, HCD, and ETD analyses using an LTQ-Orbitrap mass spectrometer (Thermo Fisher). Data were analyzed manually, yielding the N-terminal sequence as well as a shorter internal sequence fragment (<Q[L/I]RPAFCYEDPPFFQKCGAFVDSYYF… and …HFFYGQCDV…).

Partial protein sequences were used to clone full-length MitTxα and MitTxβ cDNAs. RNA was extracted from two *M. t. tener* venom glands using TRIZOL reagent (Invitrogen), then isolated by chloroform extraction and isopropanol precipitation. A cDNA library was generated for use in 5′ and 3′ RACE reactions using SMARTer RACE cDNA Amplification Kit (Clontech). Primers derived from biochemically-determined sequences and, for MitTxβ, taking advantage of conservation in reported *Micrurus* PLA2 sequences, small fragments of MitTxα and MitTxβ sequences were amplified by PCR and then used to design gene-specific 3′ and 5′RACE primers. RACE products were sequenced individually after insertion into TOPO vector (Invitrogen), and each sequence fragment was confirmed by multiple sequencing reads and multiple RACE primer sets. The cDNA-derived peptide sequence predicted the observed molecular weight of the purified toxins after consideration of the post-translational modifications (N-terminal cyclization and disulfide bond formation).

Calorimetry

MitTxα and MitTxβ were diluted into ITC buffer [(mM): 150 NaCl, 1 $CaCl_2$, 10 HEPES, adjusted to pH 7.4 with NaOH). Toxin aliquots were diluted with water prior to dilution with ITC buffer to maintain the same dilution factor. Diluted toxin solutions were centrifuged (65,000 × g for 30 min at 4 °C), degassed (5 min at 15 °C), and loaded into a VP-ITC Microcalorimeter (MicroCal). MitTxβ (3 to 10 μM) was titrated into MitTxα (0.3 to 1 μM) following a schedule of one 4μL injection followed by 29 injections of 10μL, each spaced by

5 min. Titrations were conducted at 15 °C. After manual baseline correction, total heat released per injection was calculated by integrating over the full injection time period. Heat of dilution was estimated by the final titration points and subtracted from baseline. Linear baseline values were confirmed by titration of MitTxβ into buffer. Data were processed and fit to a single-site binding model using Origin v.7 (MicroCal). Reported values are averages of three independent experiments.

Molecular Biology

Full-length (not including UTRs) ASIC1a, 1b, 2a, 3, and 4 were cloned from rat trigeminal ganglion or brain cDNA libraries into pCDNA3.1 (Invitrogen). The mouse ASIC2b clone was kindly provided by Michael Welsh (University of Iowa, IA), rat ENaC clones were provided by David Pearce (University of California, San Francisco, CA). All constructs were confirmed by DNA sequencing. Other constructs and RNA synthesis have been previously described[6].

Xenopus Oocyte and CHO/HEK Cell Culture

Xenopus laevis oocytes (Nasco), human embryo kidney 293 (HEK293), and Chinese hamster ovary (CHO-K1) cells were isolated, maintained, transfected, and plated essentially as described[6]. Oocytes were injected with RNA (3–50 ng; 50 nl), and assayed 3–7 days later. CHO culture medium included non-essential amino acids (UCSF Cell Culture Facility). Electrophysiological experiments were conducted 2-20 hours after plating, and imaging experiments were performed 3-4 hours after plating.

Neuronal Cell Culture

Trigeminal ganglia (TG) were dissected from newborn (P0-P2) Sprague-Dawley rats or C57BL/6 mice and cultured as described[6] for 3-4 hours before calcium imaging or 2-20 hours before electrophysiological recordings. Neurons dissected from newborn animals were used for all experiments except histology, which used adult neurons due to apparent developmental changes in ASIC subtype expression (see Supplementary Fig 4c). Dorsal root ganglia from adult (4-12 week old) mice were dissected and dissociated as newborn neurons except collagenase P and trypsin incubations were extended to 30 min each. After trituration, cells were centrifuged through a 15% BSA gradient for 5 min at 1000 × g to remove cellular debris. BSA was rinsed from the pellet and cells were resuspended in culture medium. Cells were plated into PDL-coated 384-well plates (Greiner Bio-One) for 14-18 hours before calcium imaging.

Calcium Imaging

Cells were loaded with Fura-2-AM as described[6]. MitTxα, MitTxβ, and PcTx1 solutions were prepared in the presence of 0.1% bovine serum albumin (BSA, Sigma) to minimize toxin adsorption to plasticware. For experiments using low concentrations of MitTxα/β, MitTxα and MitTxβ were first mixed at high concentrations (≥ 1 μM) for ≥ 10 min before dilution.

Electrophysiology

Xenopus oocyte two electrode and mammalian whole-cell recordings were carried out essentially as described[6]. Oocyte extracellular solution contained (mM): 115 NaCl, 2.5 KCl, 1.8 $MgCl_2$, 5 HEPES, and 5 MES adjusted to pH 5-7.4 with NaOH. For pH < 5 citrate was used instead of HEPES/MES. Solutions were applied using gravity-based perfusion over a small-volume oocyte chamber (Automate Scientific), except for toxin-containing solutions, which were pipetted directly onto cells.

Mammalian cell extracellular solution contained (mM): 150 NaCl, 2.8 KCl, 1 $MgCl_2$, 1 $CaCl_2$, 5 HEPES, 5 MES adjusted to pH 7.4 with NaOH, 300-310 mOsmol kg^{-1}. The pipette solution contained (mM): 130 K-gluconate, 15 KCl, 4 NaCl, 0.5 $CaCl_2$, 1 EGTA, 10 HEPES, adjusted to pH 7.2 with KOH, 285 mOsmol kg^{-1}. Solutions were applied from the micro-perfusion system SmartSquirt (Automate Scientific). Toxins were applied in the presence of 0.1 % BSA and MitTxα/β complex was formed at high concentrations as described above.

Fits to the Hill equation were performed using Igor Pro software (Wavemetrics) with four free parameters. Fits in Fig 2d revealed the following values for EC_{50}, n_H, and maximum respectively: 9.4 ± 1.3 nM, 2.4 ± 0.8, and 1.30 ± 0.08 for ASIC1a; 23 ± 1 nM, 3.6 ± 0.7, and 1.35 ± 0.05 for ASIC1b; 36 ± 4 nM, 0.088 ± 0.005, and 2.2 ± 0.5 for ASIC2a; and 830 ± 250 nM, 1.4 ± 0.3, and 1.8 ± 0.3 for ASIC3. Fits in Fig 2f revealed the following values for pH_{50}, n_H, and maximum respectively: 5.98 ± 0.07, 1.3 ± 0.3, and 0.99 ± 0.03 in the presence of toxin and 2.4 ± 0.1, 1.0 ± 0.1, and 1.6 ± 4.1 in the absence of toxin. The baseline parameter was near-zero for all fits.

For permeability experiments from acutely dissociated rat TG neurons, endogenous currents were attenuated by using a minimal ionic composition and by applying rapid voltage ramps (140 ms ramps from -80 mV to +80 mV were applied every 200 ms) to drive inactivating voltage-gated channels into a non-conductive state; extracellular and intracellular solutions contained (mM): 150 NaCl, 1 $MgCl_2$, 1 $CaCl_2$, 10 HEPES adjusted to pH 7.4 with NaOH. Remaining endogenous currents were negligible in magnitude compared to the very large MitTx-evoked currents, so no baseline subtraction was applied. Dialysis of the intracellular solution was monitored to completion as determined by elimination of K_v channel currents. Cesium wash solution contained 150 mM CsCl instead of NaCl, and pH was titrated with CsOH. P_{Na^+} / P_{Cs^+} was calculated by substituting the observed reversal potential (V_m) into the Goldman-Hodgkin-Katz voltage equation: $\frac{PNa+}{PCs+} = e^{-Vm * \frac{F}{RT}}$ where F, R, and T have their usual meanings (F/RT = 39.6 V^{-1} at 20 °C). Currents were not corrected for liquid junction potential changes.

Immunohistochemistry

After calcium imaging, adult DRG neurons were fixed with 4% paraformaldehyde (10 min) then washed 3 times in PBS containing 0.1% triton X (PBSTx). Neurons were incubated in blocking solution for 1 hour (10% normal goat serum (NGS) + PBSTx) and then incubated overnight in primary antibody solution (2.5% NGS + PBSTx + primary antibody; rabbit

anti-TRPV1, 1:8000 or mouse anti-N5A; Sigma, 1:1000). Cells were washed 3 times with PBSTx before a 2-hour incubation in secondary antibody solution (2.5% NGS + PBSTx, + Alexa-488 or Alexa-594; Invitrogen, 1:1000). For IB4 staining, IB4-FITC (Sigma, 10 μg ml^{-1}) was added to the secondary antibody solution. Cells were washed 3 times in PBS before imaging.

For spinal cord Fos immunoreactivity, mice were perfused transcardially with 4% paraformaldehyde 90 min after hindpaw toxin injection (as for behavioral experiments). Frozen spinal cord sections (25 μm) were prepared from lumbar level L4/L5 and immunostained for Fos as described[29].

Behavior

Animal experiments were approved by the UCSF Institutional Animal Care and Use Committee and conducted in accordance with the National Institutes of Health (NIH) Guide for the Care and Use of Laboratory Animals and the recommendations of the International Association for the Study of Pain. Two to five animals were housed per cage and maintained on a 12-h light/dark schedule with ad lib access to food and water. Injections (20 μL of PBS + 0.1% BSA, with or without 5 μM MitTx) were performed as described[5]. For intrathecal capsaicin studies, adult were anesthetized and treated as described[21]. Behavioral tests were performed 1 to 5 days after capsaicin injection. Knockout strains were extensively backcrossed to the C57BL/6 wildtype strain. Both behavioral and histological experiments were conducted and scored with the experimenter blind to genotype.

Primer sequences

MitTxβ Fragment forward: AACCTCTAYCAGTTCATGATTAAATGTACCAACG

MitTxβ Fragment reverse: TCATTGGCAACGTTTGAGGTCGATATTG

MitTxβ 3′RACE: GTTATCTAGCCAGCGACCTCGATTGCAGTGG

MitTxβ 5′RACE: CCACTGCAATCGAGGTCGCTGGCTAGATAAC

MitTxα fragment forward: CCNCCNTTYTTYCARAARTGYGGNGCNTTYGTNG

MitTxα fragment reverse: ACRTCRCAYTGNCCRTARAARAARTG

MitTxα 3′RACE: CCTCCATTCTTTCAAAAATGTGGAGCC

MitTxα 5′RACE: CGCAAGTAATTCTTGACCTGTTGAAGTAGTAGG

Supplementary Material

Refer to Web version on PubMed Central for supplementary material.

Acknowledgments

We thank M. Price and M. Welsh for kindly providing ASIC1 and ASIC3 knockout mice; Y. Kelly and J. Poblete for technical assistance; C. Williams for assisting with homology models; F. Findeisen, L. Ma, and D. Minor for assistance with ITC experiments; R. Nicoll and members of the Julius lab for discussion and critical comments.

This work was supported by a Ruth Kirschstein NIH predoctoral fellowship (F31NS065597 to C.B.), NIH postdoctoral training grant from the UCSF Cardiovascular Research Institute (A.C.), postdoctoral fellowship from the Canadian Institutes of Health Research (R.S-N.), the Howard Hughes Medical Institute (K.F.M. and A.L.B.), and the NIH (NCRR P41RR001614 to A.L.B., NCRR P40RR018300-09 to E.S., and NINDS R01NS065071 to D.J.).

References

1. Basbaum AI, Bautista DM, Scherrer G, Julius D. Cellular and molecular mechanisms of pain. Cell. 2009; 139:267–284. [PubMed: 19837031]
2. Mebs, D. Venomous and poisonous animals : a handbook for biologists, and toxicologists and toxinologists, Physicians and pharmacists. CRC Press; 2002.
3. Chahl LA, Kirk EJ. Toxins which produce pain. Pain. 1975; 1:3–49. [PubMed: 800636]
4. Schmidt JO. Biochemistry of insect venoms. Annu Rev Entomol. 1982; 27:339–368. [PubMed: 7044266]
5. Siemens J, et al. Spider toxins activate the capsaicin receptor to produce inflammatory pain. Nature. 2006; 444:208–212. [PubMed: 17093448]
6. Bohlen CJ, et al. A bivalent tarantula toxin activates the capsaicin receptor, TRPV1, by targeting the outer pore domain. Cell. 2010; 141:834–845. [PubMed: 20510930]
7. Terlau H, Olivera BM. Conus venoms: a rich source of novel ion channel-targeted peptides. Physiol Rev. 2004; 84:41–68. [PubMed: 14715910]
8. Fry BG, et al. The toxicogenomic multiverse: convergent recruitment of proteins into animal venoms. Annu Rev Genomics Hum Genet. 2009; 10:483–511. [PubMed: 19640225]
9. Morgan DL, Borys DJ, Stanford R, Kjar D, Tobleman W. Texas coral snake (Micrurus tener) bites. South Med J. 2007; 100:152–156. [PubMed: 17330685]
10. Doley R, Kini RM. Protein complexes in snake venom. Cell Mol Life Sci. 2009; 66:2851–2871. [PubMed: 19495561]
11. Berg OG, Gelb MH, Tsai MD, Jain MK. Interfacial enzymology: the secreted phospholipase A(2)-paradigm. Chem Rev. 2001; 101:2613–2654. [PubMed: 11749391]
12. Waldmann R, Champigny G, Bassilana F, Heurteaux C, Lazdunski M. A proton-gated cation channel involved in acid-sensing. Nature. 1997; 386:173–177. [PubMed: 9062189]
13. Waldmann R, et al. Molecular cloning of a non-inactivating proton-gated Na+ channel specific for sensory neurons. J Biol Chem. 1997; 272:20975–20978. [PubMed: 9261094]
14. Wu LJ, et al. Characterization of acid-sensing ion channels in dorsal horn neurons of rat spinal cord. J Biol Chem. 2004; 279:43716–43724. [PubMed: 15302881]
15. Escoubas P, et al. Isolation of a tarantula toxin specific for a class of proton-gated Na+ channels. J Biol Chem. 2000; 275:25116–25121. [PubMed: 10829030]
16. Chen X, Kalbacher H, Grunder S. Interaction of acid-sensing ion channel (ASIC) 1 with the tarantula toxin psalmotoxin 1 is state dependent. J Gen Physiol. 2006; 127:267–276. [PubMed: 16505147]
17. Leffler A, Monter B, Koltzenburg M. The role of the capsaicin receptor TRPV1 and acid-sensing ion channels (ASICS) in proton sensitivity of subpopulations of primary nociceptive neurons in rats and mice. Neuroscience. 2006; 139:699–709. [PubMed: 16515841]
18. Poirot O, Berta T, Decosterd I, Kellenberger S. Distinct ASIC currents are expressed in rat putative nociceptors and are modulated by nerve injury. J Physiol. 2006; 576:215–234. [PubMed: 16840516]
19. Price MP, et al. The DRASIC cation channel contributes to the detection of cutaneous touch and acid stimuli in mice. Neuron. 2001; 32:1071–1083. [PubMed: 11754838]
20. Wemmie JA, et al. The acid-activated ion channel ASIC contributes to synaptic plasticity, learning, and memory. Neuron. 2002; 34:463–477. [PubMed: 11988176]
21. Cavanaugh DJ, et al. Distinct subsets of unmyelinated primary sensory fibers mediate behavioral responses to noxious thermal and mechanical stimuli. Proc Natl Acad Sci U S A. 2009; 106:9075–9080. [PubMed: 19451647]

22. Nishioka SA, Silveira PV, Menzes LB. Coral snake bite and severe local pain. Ann Trop Med Parasitol. 1993; 87:429–431. [PubMed: 8250638]
23. Sutherland SP, Benson CJ, Adelman JP, McCleskey EW. Acid-sensing ion channel 3 matches the acid-gated current in cardiac ischemia-sensing neurons. Proc Natl Acad Sci U S A. 2001; 98:711–716. [PubMed: 11120882]
24. Wemmie JA, Price MP, Welsh MJ. Acid-sensing ion channels: advances, questions and therapeutic opportunities. Trends Neurosci. 2006; 29:578–586. [PubMed: 16891000]
25. Deval E, et al. Acid-sensing ion channels (ASICs): pharmacology and implication in pain. Pharmacol Ther. 2010; 128:549–558. [PubMed: 20807551]
26. Yu Y, et al. A nonproton ligand sensor in the acid-sensing ion channel. Neuron. 2010; 68:61–72. [PubMed: 20920791]
27. Ziemann AE, et al. The amygdala is a chemosensor that detects carbon dioxide and acidosis to elicit fear behavior. Cell. 2009; 139:1012–1021. [PubMed: 19945383]
28. Askwith CC, et al. Neuropeptide FF and FMRFamide potentiate acid-evoked currents from sensory neurons and proton-gated DEG/ENaC channels. Neuron. 2000; 26:133–141. [PubMed: 10798398]
29. Caterina MJ, et al. Impaired nociception and pain sensation in mice lacking the capsaicin receptor. Science. 2000; 288:306–313. [PubMed: 10764638]
30. Jacobson MP, et al. A hierarchical approach to all-atom protein loop prediction. Proteins. 2004; 55:351–367. [PubMed: 15048827]

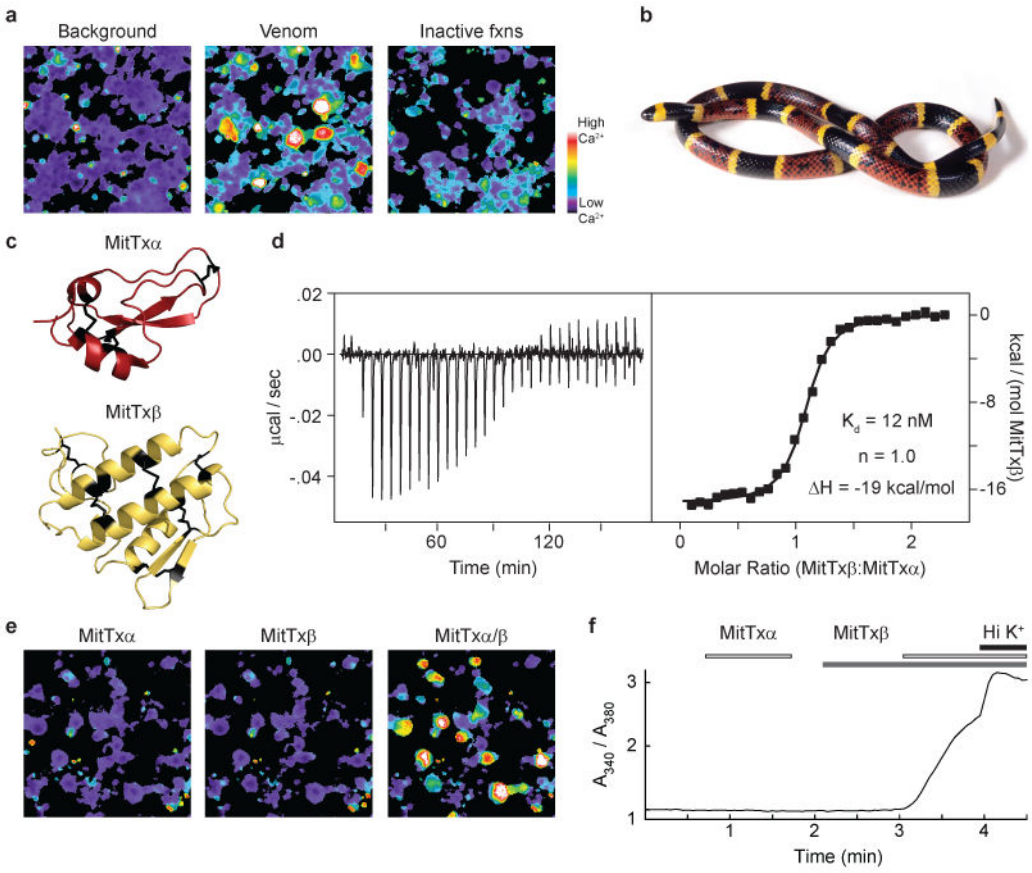

Figure 1. Heteromeric toxin from Texas coral snake activates somatosensory neurons

a, *M. t. tener* venom (0.1 mg ml^{-1}) activates acutely dissociated trigeminal ganglion (TG) neurons as assessed by ratiometric calcium imaging. Pooled venom fractions lacking neuron-specific activity (inactive fxns) produced only weak signals in non-neuronal cells (color bar indicates relative calcium levels). **b**, The Texas coral snake. **c**, Homology-based predicted structural models of MitTx subunits, generated using Prime (Schrodinger)[30]. **d**, Isothermal titration calorimetry reveals formation of high-affinity MitTxα/β complex with 1:1 stoichiometry. **e**, MitTxα and MitTxβ have no effect individually, but recapitulate activity of whole venom when applied together to TG neurons. **f**, Average calcium response from >100 randomly-selected TG neurons that also responded to high extracellular potassium (Hi K^+, 100 mM KCl). Activation by MitTxα/β (300 nM each) only occurs when both toxins are present.

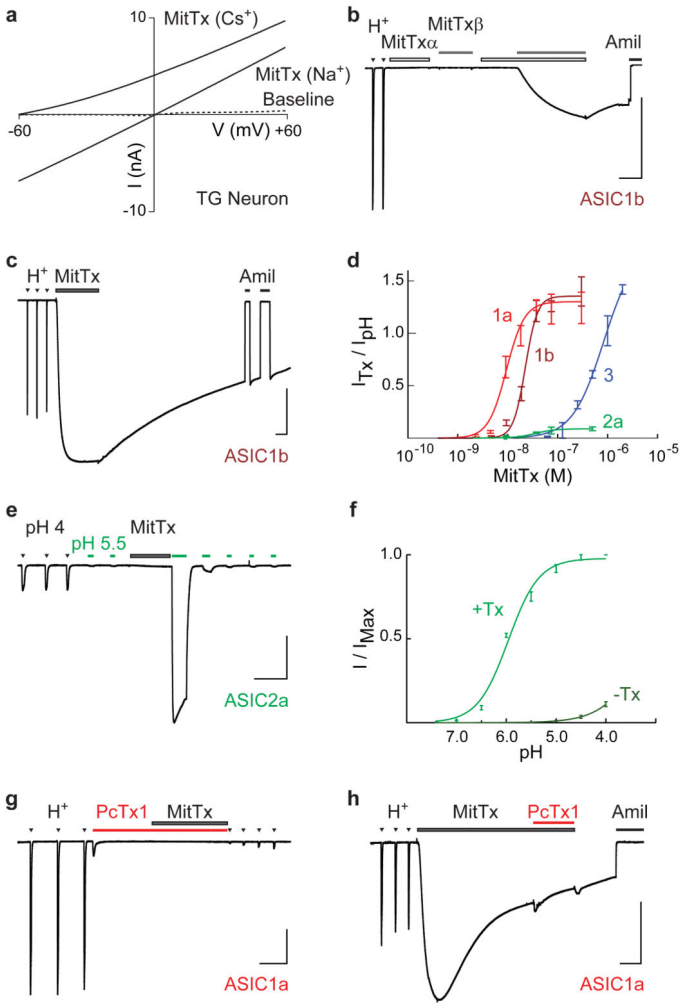

Figure 2. MitTx activates ASICs

a, Current-voltage relationships of MitTx (300 nM)-evoked conductances from TG neurons (whole-cell configuration) demonstrate higher permeability for Na^+ over Cs^+. The intracellular solution contained 150 mM Na^+, and a leftward-shift in the reversal potential was observed when the major extracellular cation was changed from 150 mM Na^+ to 150 mM Cs^+. **b**, Voltage clamp recordings show that ASIC1b-expressing oocytes respond to both extracellular acidification (H^+, pH 4) and MitTx, but are insensitive to MitTxα (30 nM) or MitTxβ (300 nM) individually. Toxin-evoked responses were blocked by amiloride (Amil, 1mM). **c**, MitTx (75 nM)-evoked currents are comparable in magnitude to pH 4-evoked currents in ASIC1b-expressing oocytes. Toxin responses are non-desensitizing and persistent compared to transient proton-evoked currents. **d**, Dose-response analysis of toxin-evoked currents normalized to maximal pH 4-evoked response in ASIC-expressing oocytes. Data were fit to the Hill equation. **e**, MitTx (75 nM) is a poor ASIC2a agonist, but dramatically potentiates pH 5.5-evoked responses. **f**, pH dose-response of ASIC2a in the absence (dark green) or presence (light green) of 75 nM MitTx. Data were fit to the Hill equation. **g**, PcTx1 (100 nM) inhibits both pH 6- and MitTx-evoked currents in ASIC1a-

expressing oocytes. **h**, MitTx occludes PcTx1 inhibition. Vertical scale bars: 1μA; horizontal bars: 1 min; V_h = -60 mV.

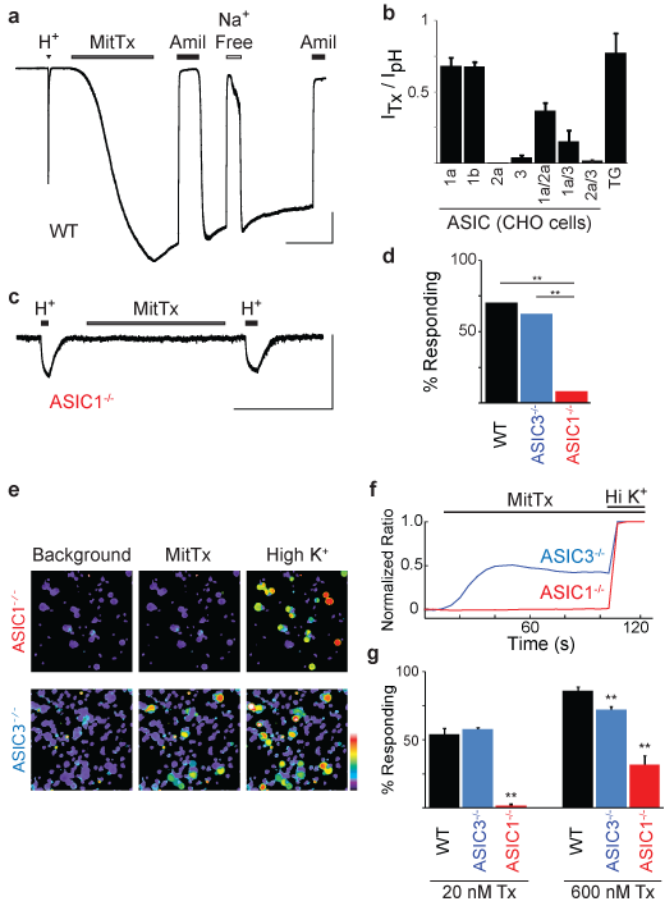

Figure 3. ASICs are the neuronal receptor for MitTx

a, Whole-cell recording (V_h = -60 mV) from newborn rat TG neuron shows representative pH 4 (H^+)- and MitTx (75 nM)-evoked responses. Toxin responses were blocked by amiloride (Amil; 1 mM), and eliminated when extracellular Na^+ was replaced with Cs^+ (Na^+ Free). **b**, MitTx (75 nM) activates homo- and heteromeric ASIC family members expressed in CHO cells. MitTx to pH current ratios for ASIC1a or 1b (n = 3-6) resembled profile observed in TG neurons (n = 28). pH 4 was used for all ratios except for measurements of ASIC1a, in which case pH 6 was used to minimize tachyphylaxis. **c**, TG neurons from newborn ASIC1$^{-/-}$ mice lacked MitTx sensitivity. H^+ indicates pH 4. **d**, Percentage of wild type or knockout TG neurons in which toxin-evoked currents were observed by whole cell patch clamp analysis (n = 10-30, **p < 0.01, chi-squared test). **e**, MitTx (20 nM) activates TG neurons from ASIC3$^{-/-}$, but not ASIC1$^{-/-}$ mice. **f**, Average MitTx-evoked calcium response of TG neurons (n > 300) normalized to a high-potassium response (Hi K^+). **g**, Fraction of neurons responding to 20 nM or 600 nM MitTx assessed by calcium imaging (n = 3-4 trials, each with > 100 cells; ** p < 0.01, one-way ANOVA with *post hoc* Tukey's test) Vertical scale bars: 1nA in **a**, 100 pA in **b**. Horizontal scale bars: 1 min. Error bars represent mean ± sem.

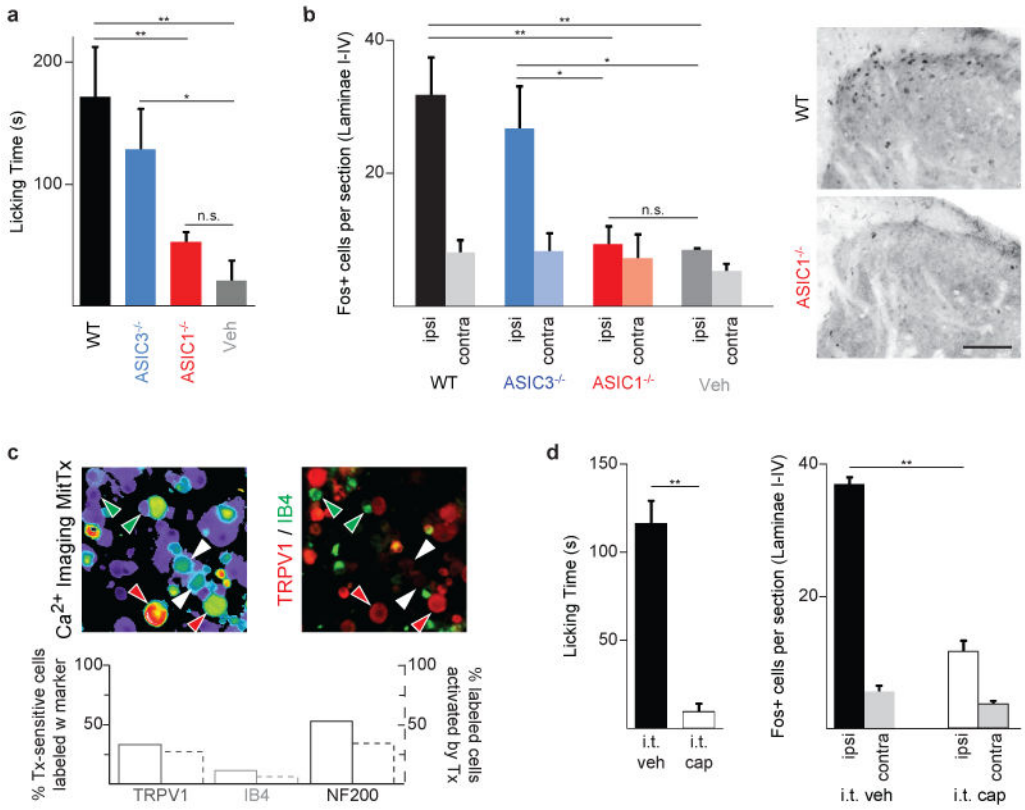

Figure 4. MitTx elicits pain behavior via ASIC1- and TRPV1-expressing nociceptors

a, Hind paws of wild-type (WT) or ASIC-knockout mice were injected with MitTx (5 μM in 20 μl PBS with 0.1% BSA) or vehicle alone. Total time spent licking the injected paw was recorded over 15 min. **b**, Quantification and representative images of Fos immunostaining in superficial laminae of spinal cord sections from toxin-injected mice (ipsilateral or contralateral to the injection site). Scale bar: 50 μm. For **a** and **b**, n = 4-7; *p < 0.05; **p < 0.01, one-way ANOVA with *post hoc* Tukey's test. **c**, Adult mouse DRG neurons were tested for toxin-sensitivity using calcium imaging, then stained with antibodies that mark specific subpopulations of cells. Red arrows: Tx-sensitive/TRPV1-positive cells; white arrows: Tx-sensitive/TRPV1-negative cells; green arrows, IB4-positive/Tx-insensitive cells. Percentages were counted for >200 cells per marker and graphed below. **d**, Intrathecal administration of capsaicin (i.t. cap, 10 μg in 5 μl), but not vehicle, eliminates behavioral response and spinal Fos induction after intraplantar toxin injection (as in **a, b**). n = 3–4; **p < 0.001, Student's t-test. Error bars represent mean ± sem.